Human Molecular Genetics, 2010, Vol. 19, No. 22 **4399–4408**
doi:10.1093/hmg/ddq363
Advance Access published on September 3, 2010

Kinesin-1 transport reductions enhance human tau hyperphosphorylation, aggregation and neurodegeneration in animal models of tauopathies

Tomás L. Falzone[†], Shermali Gunawardena[‡], David McCleary, Gerald F. Reis[¶] and Lawrence S.B. Goldstein[*]

Department of Cellular and Molecular Medicine, Howard Hughes Medical Institute, University of California, San Diego, La Jolla, CA 92093, USA

Received April 19, 2010; Revised and Accepted August 20, 2010

Neurodegeneration induced by abnormal hyperphosphorylation and aggregation of the microtubule-associated protein tau defines neurodegenerative tauopathies. Destabilization of microtubules by loss of tau function and filament formation by toxic gain of function are two mechanisms suggested for how abnormal tau triggers neuronal loss. Recent experiments in kinesin-1 deficient mice suggested that axonal transport defects can initiate biochemical changes that induce activation of axonal stress kinase pathways leading to abnormal tau hyperphosphorylation. Here we show using *Drosophila* and mouse models of tauopathies that reductions in axonal transport can exacerbate human tau protein hyperphosphorylation, formation of insoluble aggregates and tau-dependent neurodegeneration. Together with previous work, our results suggest that non-lethal reductions in axonal transport, and perhaps other types of minor axonal stress, are sufficient to induce and/or accelerate abnormal tau behavior characteristic of Alzheimer's disease and other neurodegenerative tauopathies.

INTRODUCTION

Neurodegenerative tauopathies are a group of neuronal disorders characterized by abnormal hyperphosphorylation and accumulation of the microtubule-associated tau protein into intracellular insoluble inclusions called neurofibrillary tangles (NFTs) (1–3). Tau abnormalities in Alzheimer's disease (AD), frontotemporal dementias (FTDs) and other tau linked diseases are accompanied by synaptic failure, transport defects, protein aggregation and neuronal loss (4–7). The discovery of mutations in the human gene encoding tau protein established that dysfunction of tau by itself can cause neurodegeneration and dementia (8–10). While tauopathies differ in cell type and brain region affected, the hyperphosphorylation of tau by diverse kinases appears to cause microtubule destabilization and formation of filament pathologies (11–14). Loss and toxic gain of tau function are suggested to impair axonal transport mechanisms causing disease (4,15,16).

Tau protein has long been thought to play key roles in axonal transport, which is essential in long polarized neurons for delivery of proteins, vesicles and organelles to support synaptic function (16). Molecular motors such as kinesin and dynein transport cargos along microtubules in the anterograde and retrograde direction, respectively. Tau overexpression can impair the axonal localization of vesicles and proteins by inhibiting kinesin-dependent transport (17). *In vitro* experiments suggested that the amount of tau associated with microtubules can differentially modulate kinesin and dynein activities (18). Moreover, tau phosphorylation can regulate its association with motor machinery suggesting that signaling deregulation events can lead to tau mislocalization (19).

Both the somatodendritic and axonal accumulation of tau are closely associated with axonopathies in tau diseases (5). Expression of human wild-type and mutant tau in *Drosophila* causes neurodegeneration in the absence of tau filaments, suggesting that tau overexpression alone can induce neuronal

[*]To whom correspondence should be addressed at: University of California, San Diego, 9500 Gilman Dr, Leichtag Biomedical Research Building, La Jolla, CA 92093-0683, USA. Tel: +1 8585349702; Fax: +1 8585348193; Email: lgoldstein@ucsd.edu
[†]Present address: Instituto de Biología Celular y Neurociencia, Facultad de Medicina, Universidad de Buenos Aires, Buenos Aires, Argentina.
[‡]Present address: Department of Biological Sciences, The State University of New York at Buffalo, Buffalo, NY 14260, USA.
[¶]Present address: Department of Pathology, University of California San Francisco, San Francisco, CA 94143, USA.

death (20,21). The transgenic expression of human mutant tau protein P301L, found in some types of FTDP-17, recapitulates in mouse a number of disease phenotypes such as the formation of NFTs (22,23). Moreover, abnormal neuronal tau localization and aggregation in transgenic mice have been suggested to be caused by retarded transport of the P301L tau protein (24).

Motor protein mutations can also give rise to different types of neurodegenerative diseases that exhibit axonal cargo accumulation in swellings and axonopathies (16). Neuronal tracing in living mice carrying a deletion of the kinesin light chain 1 (KLC1−/−) motor subunit revealed delayed axonal transport rates (25). Interestingly, recent experiments in KLC1−/− mice suggested that early and selective transport defects can activate c-Jun N-terminal stress kinase (JNK) pathways that initiate abnormal hyperphosphorylation of tau in the absence of Aβ toxicity (26). These experiments did not, however, reveal whether transport reduction can exacerbate the progression of the inherently pathogenic human tau abnormal hyperphosphorylation or aggregation in tauopathies. Because mouse tau protein cannot form classic tau filaments or NFTs, here we tested whether kinesin-1 transport reduction can enhance abnormal tau phenotypes that are typical of human tau protein. Therefore, we induced KLC reductions in *Drosophila* and mouse overexpressing human wild-type or mutated tau protein to test for exacerbation of tau aggregation and neurodegeneration in animal models of tauopathies.

RESULTS

Elevated human tau accumulation, hyperphosphorylation and tau-mediated neurotoxicity induced by KLC reduction in *Drosophila*

Neuronal expression of human wild-type (tau^{wt}) or mutant tau (tau^{R406W}) in *Drosophila* causes some features of human tauopathies including accumulation of abnormal tau, progressive neurodegeneration and early death, but without NFTs (20). To test whether reduction in axonal transport can enhance these phenotypes in a *Drosophila* tauopathy model, we combined a genetic reduction of the kinesin light chain (KLC) subunit of kinesin-1 with expression of human tau^{wt} or tau^{R406W}. Consistent with previous reports (27), we found that neuron-specific expression of either tau^{wt} or tau^{R406W} using the Appl/Gal4-UAS system in *Drosophila* larvae induced substantial axonal vesicle accumulations (Fig. 1A and B). To reduce KLC protein content by 50%, we used the KLC^{8ex94} null allele in combination with expression of human tau^{wt} or tau^{R406W}. Control viability data were obtained by mating wild-type females with males carrying the X-linked ApplGal4 driver and KLC^{8ex94}/T(2,3)B3 (Supplementary Material, Fig. S1a). When UAS-tau^{wt} or UAS-tau^{R406W} transgenic flies were crossed to ApplGal4;KLC^{8ex94}/T(2,3)B3 flies to reduce KLC, we found a dramatic enhancement in tau-induced mortality (Fig. 1C; Supplementary Material, Fig. S1b and c). We observed a significant reduction (30–40%) in the viability of animals expressing either tau^{wt} or tau^{R406W} with reduced KLC when compared with tau^{wt} or tau^{R406W} alone, respectively (Fig. 1C). To test for abnormal tau protein accumulation when axonal transport is reduced, we performed quantitative western blots from brains of surviving adults carrying KLC reductions combined with tau^{wt} or tau^{R406W} (tau^{wt};$KLC^{+/8ex94}$, tau^{R406W};$KLC^{+/8ex94}$) and compared them to brains of adult flies expressing tau^{wt} or tau^{R406W} alone (Fig. 1D). Increased total tau (Tau-5, 2.5–3-fold) and elevated accumulation of phosphorylated forms of tau at Ser 202 (CP13, 3–3.5-fold) and Ser 396/404 (PHF-1, 2–2.5-fold) were observed after reducing *KLC* gene dose in flies expressing human tau^{wt} or tau^{R406W} (Fig. 1D and E). Interestingly, in these flies, we also observed significantly more activated JNK (p-JNK, 1.7–2-fold) together with observed tau accumulation (Fig. 1E). In control experiments, tau overexpression in a different genetic background with wild-type amounts of KLC (tau^{wt}/B3 or tau^{R406W}/B3) showed no increase in p-JNK and had similar phosphorylated tau levels compared with tau^{wt} or tau^{R406W} (Supplementary Material, Fig. S2). Thus, reduction in kinesin-1-dependent axonal transport in *Drosophila* stimulates enhanced neuronal stress kinase activation and abnormal tau phosphorylation and stabilization leading to an increase in tau-mediated neurodegeneration, independent of NFTs.

Age-dependent tau hyperphosphorylation is enhanced by transport reduction in the hippocampus and spinal cord of tau P301L mice

The cell body accumulation of hyperphosphorylated tau is an abnormal phenotype observed in AD and other neurodegenerative tauopathies (3,28,29). The transgenic expression of four repeat human tau harboring the P301L mutation under the prion promoter in mouse recapitulates the progressive cell body accumulation of tau phosphorylated at sites such as Ser 202 (CP13) (22,29). This early pathology is associated with the appearance of axonopathies in mice and is dependent on mutant protein amount (30,31). To test whether transport defects can exacerbate abnormal tau hyperphosphorylation in mice expressing one copy of the P301L tau mutation (tau^{P301L}), we reduced KLC1 protein by 50% (KLC1+/−). Tau^{P301L};KLC1+/− mice were born in the expected proportion and did not show changes in body weight. To characterize age-dependent pathologies in the brain, we performed immunohistochemical staining for phosphorylated tau (CP13) in hippocampal sections from tau^{P301L} mice with or without reduction in KLC1 (Fig. 2A and C). As animals aged, comparison of mice with or without KLC1 reduction revealed differences in the amount of phosphorylated Ser 202 present in the dentate gyrus and the CA1 region of the hippocampus (Fig. 2B and D). Surprisingly, at 9 months of age, the dentate gyrus of tau^{P301L};KLC1+/− showed a significant increase in CP13 positive cell bodies compared with dentate gyrus of tau^{P301L};KLC1+/+ mice (Fig. 2B). Similarly, in CA1, tau^{P301L};KLC1+/− showed higher number of CP13 cell bodies compared with tau^{P301L};KLC1+/+ at 9 months of age (Fig. 2D). We observed an initial increase in the number of cells accumulating CP13 staining in the hippocampus followed by a significant decline at older time points for both genotypes. This result is similar to what was described in another comparable mouse model expressing the human P301L mutation under the Thy1.2 promoter (32). It is possible that neuronal cell loss at advanced ages causes the observed reduction in hippocampal Ser 202 phosphorylation and may also mask the differences between tau^{P301L};KLC1+/+ and tau^{P301L};KLC1+/− at older time points (Fig. 2B and D). It

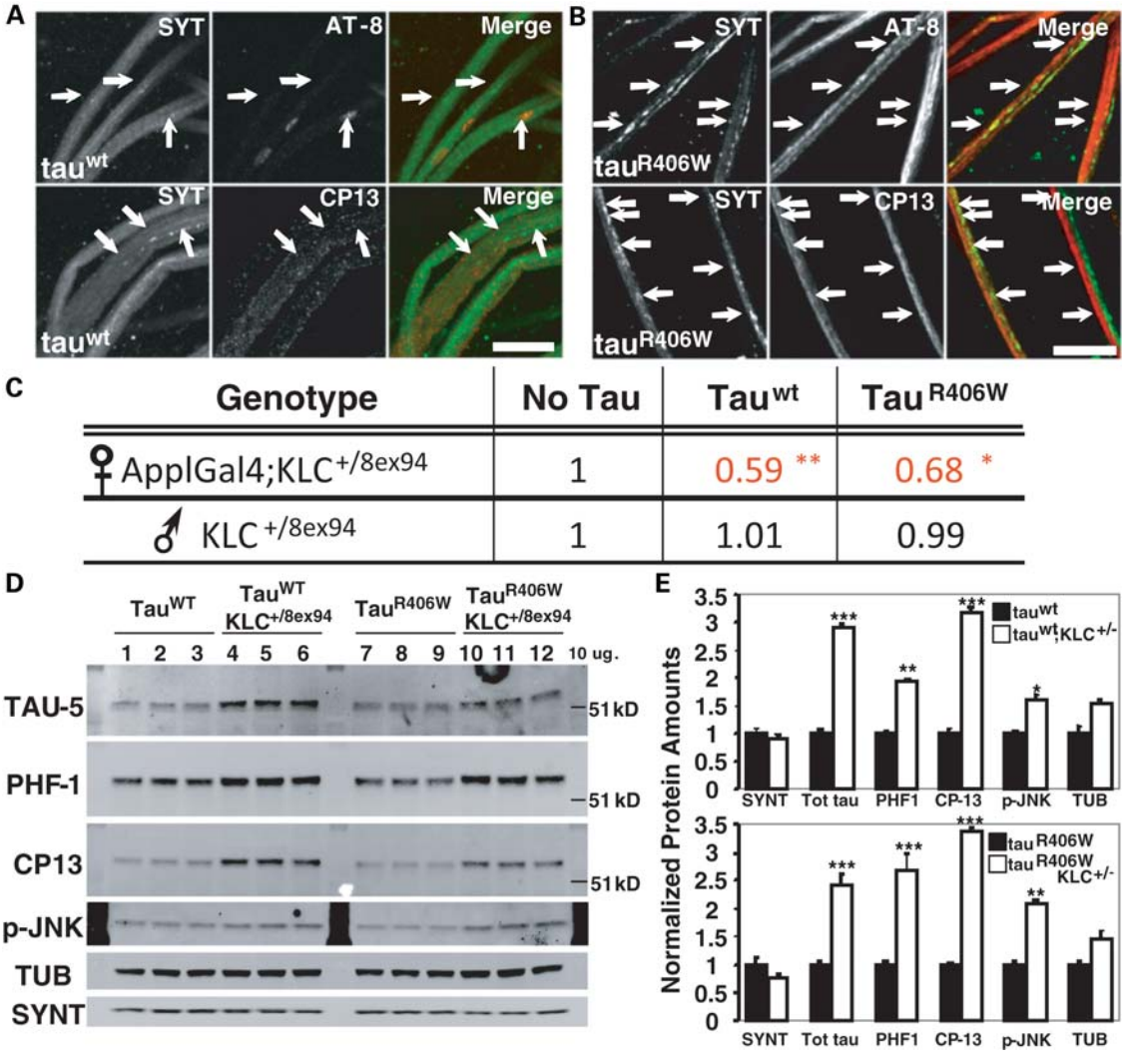

Figure 1. Axonal transport reduction exacerbates tau-mediated neurotoxicity, tau accumulation and hyperphosphorylation in *Drosophila*. (**A** and **B**) Axonal phenotypes (arrows) after staining for synaptotagmin (SYT) and phospho-tau (AT8, CP13) in nerves of ApplGal4 larvae driving the neuronal expression of human tau^{wt} (A) and tau^{R406W} (B). Scale bar=10 μm. (**C**) Relative viability table showing survival reductions in ApplGal4;$KLC^{+/8ex94}$ females expressing either tau^{wt} or tau^{R406W}. Data were normalized to female and male ratios obtained from ApplGal4;klc^{8ex94}/T(2:3)B3 crossed to WT flies. Males lacking the ApplGal4 driver were used as controls within (tau^{wt} or tau^{R406W}) and between (no tau) crosses. Moderate tau expression was obtained by performing experiments at 25°C, as opposed to stronger expression observed at 29°C. Chi-square test; no tau $n = 188$, $tau^{wt} = 355$ and $tau^{R406W} = 588$ surviving adults. $^{**}P < 0.02$, $^{*}P < 0.05$. (**D**) Western blots from 12 adult *Drosophila* head homogenates. Note the stabilization of total (TAU-5) and phosphorylated forms of tau (PHF-1, CP13) protein in tau^{wt};$KLC^{+/8ex94}$ (4–6) and tau^{R406W};$KLC^{+/8ex94}$ (10–12) compared with each control. Tubulin (TUB) and syntaxin (SYNT) were used as loading controls. (**E**) Average protein quantification from western blots using fluorescent secondary antibodies comparing TAU-5, PHF-1, CP13, p-JNK and TUB in tau^{wt} (top) and tau^{R406W} (bottom) animals. SYNT was used for normalization. Protein levels in tau^{wt};$KLC^{+/8ex94}$ and tau^{R406W};$KLC^{+/8ex94}$ (white bars) were plotted against tau^{wt} and tau^{R406W} (black bars) which were normalized to 1. An approximately 2-fold increase in tau stabilization was observed after KLC reduction in adult tau transgenic flies. Student's *t*-test; $n = 3$, $^{*}P < 0.05$, $^{**}P < 0.02$, $^{***}P < 0.01$.

is interesting that tau^{P301L};KLC1+/− always showed a qualitatively higher CP13 staining intensity compared with tau^{P301L};KLC1+/+, suggesting that elevated amounts of hyperphosphorylated tau accumulate within neurons with kinesin-1 transport reductions (Fig. 2A and C).

Because tau pathologies were prominently observed in the spinal cord of mouse tauopathy models such as tau^{P301L} (22,23), we also performed immunohistochemical staining to compare CP13 staining in cervical spinal cord sections (Fig. 3A). Stereological quantification of abnormal cell bodies in gray matter of the spinal cord revealed a progressive increase in tau pathology as animals aged with an increase for both tau^{P301L};KLC1+/+ and tau^{P301L};KLC1+/−. In the spinal cord, the regression fit for tau^{P301L};KLC1+/− revealed a higher rate of hyperphosphorylated tau accumulation compared with tau^{P301L};KLC1+/+ (Fig. 3B). Interestingly, the enhancement in CP13 accumulation in tau^{P301L};KLC1+/− compared with tau^{P301L};KLC1+/+ was maintained at older time points (Fig. 3B). These results suggest that kinesin-1 transport reduction enhances the progression and accumulation of hyperphosphorylated human tau within cell bodies of tau^{P301L} transgenic mice.

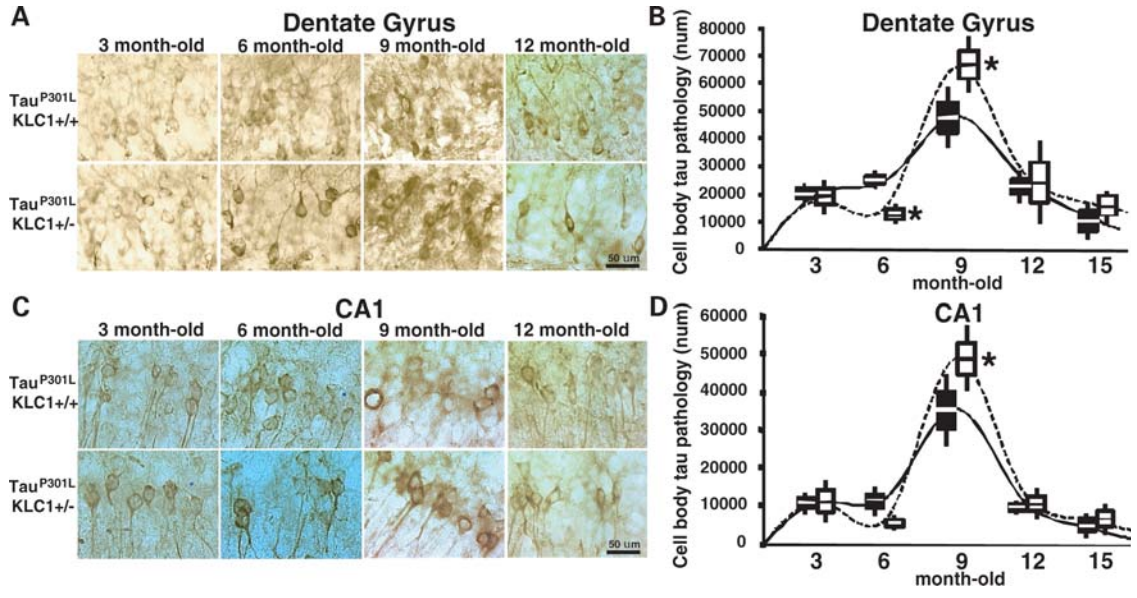

Figure 2. Increased cell body pathology in brains of KLC1 reduction combined with tau P301L. (**A** and **C**) Staining of phosphorylated tau using CP13 antibody. Neuronal cell bodies with abnormal p-tau accumulation are shown for dentate gyrus (A) and CA1 (C) region of the hippocampus in 3-, 6-, 9- and 12-month-old tau^{P301L};KLC1+/+ and tau^{P301L};KLC1+/− mice. (**B** and **D**) Stereological quantification of neuron numbers showing p-tau cell body accumulation in dentate (B) and CA1 (D) hippocampus for tau^{P301L};KLC1+/+ (black) and tau^{P301L};KLC1+/− (27). Distribution of the average number is plotted. Boxes and bars correspond to SEM and STDEV, respectively. Mann–Whitney, non-parametric test; $n = 4$, $^{*}P < 0.05$.

Age-dependent insoluble hyperphosphorylated tau accumulation is exacerbated by axonal transport reduction in the brain and spinal cord of mouse models of tauopathies

Hyperphosphorylation leads to tau detachment from microtubules and aggregation of insoluble tau into pathological NFTs in cell bodies and dystrophic neurites (1). Insoluble aggregated tau evolves to form abnormal filaments that are associated with neurodegeneration, and has been suggested as a cause of impaired neuronal function by physically obstructing neurites (5). Filamentous inclusions correlate with the appearance of insoluble tau proteins of 64 kDa or higher molecular weights in human AD and in neuronal tissue of tau^{P301L} mice (22,33). Recent experiments analyzing KLC1−/− mutant mice suggested that transport defects can trigger abnormal tau phosphorylation and aggregation (26). However, it was not determined whether transport defects can increase tau insolubility. Despite sequence similarities, endogenous tau in the mouse, unlike the human protein, has minimal tendency to form abnormal filaments or even classical NFTs (23,34). However, mice expressing tau^{P301L} contain most of the features of human neurofibrillary pathology and, more importantly, also show significant neuronal loss in affected brain regions indicating that immunoreactive NFTs are closely linked to neurodegeneration (22,35).

To test whether transport reduction can exacerbate the accumulation of insoluble human tau, we performed sarkosyl extractions of cortex, brain stem and spinal cord at different ages in tau^{P301L} tauopathy animals with and without KLC1 reduction. At 6 months of age, we found similar protein levels of total and hyperphosphorylated tau in brain cortex, brain stem and spinal cord when tau^{P301L};KLC1+/+ homogenates were compared with tau^{P301L};KLC1+/− (Supplementary Material, Fig. S3). Cortex, brain stem and spinal cord tissue from tau^{P301L};KLC1+/+ and tau^{P301L};KLC1+/− were fractionated into homogenate (H1), low salt extractable (S1) and sarkosyl-insoluble (P3) fractions. Equivalent amounts of total proteins were loaded for homogenates and soluble fractions; and equivalent volumes were loaded for insoluble fractions (33). After sarkosyl extraction, similar total tau levels in H1, S1 and P3 brain stem fractions were observed for young tau^{P301L};KLC1+/+ and tau^{P301L};KLC1+/− mice (Fig. 4A). Hyperphosphorylated tau levels in H1, S1 and P3 sarkosyl fractions (Ser 202: CP13, and Ser 396/404: PHF1) at 6 months of age were also equivalent between tau^{P301L};KLC1+/+ and tau^{P301L};KLC1+/− (Fig. 4A). Tau proteins of 64 kDa molecular weight were enriched in insoluble fractions (P3) compared with lower tau species in both genotypes (Fig. 4A and B). However, enhanced age-dependent increases of the 64 kDa insoluble hyperphosphorylated tau were found in the brain stem of tau^{P301L} mice with 50% reduction in KLC1 when compared with tau^{P301L} mouse alone (Fig. 4A). Integrated intensity quantification of the insoluble forms (P3) normalized to the amount of homogenate tau (H1) revealed a significant enhancement of insoluble tau in tau^{P301L};KLC1+/− compared with tau^{P301L};KLC1+/+ at 12 months of age (Fig. 4B). Interestingly, total and hyperphosphorylated tau levels in homogenates are similar in 12-month-old tissue in both genotypes, suggesting that in mice with transport defects more insoluble tau accumulates with age (Fig. 4B). Aberrant insoluble tau enhancements in aged mice also correlate with increased activation of JNK in tau^{P301L};KLC1+/− (Fig. 4A). Classical NFTs were observed after modified Gallyas silver staining in 12-month-old tau^{P301L};KLC1+/+ and tau^{P301L};KLC1+/− brains (Supplementary Material, Fig. S4).

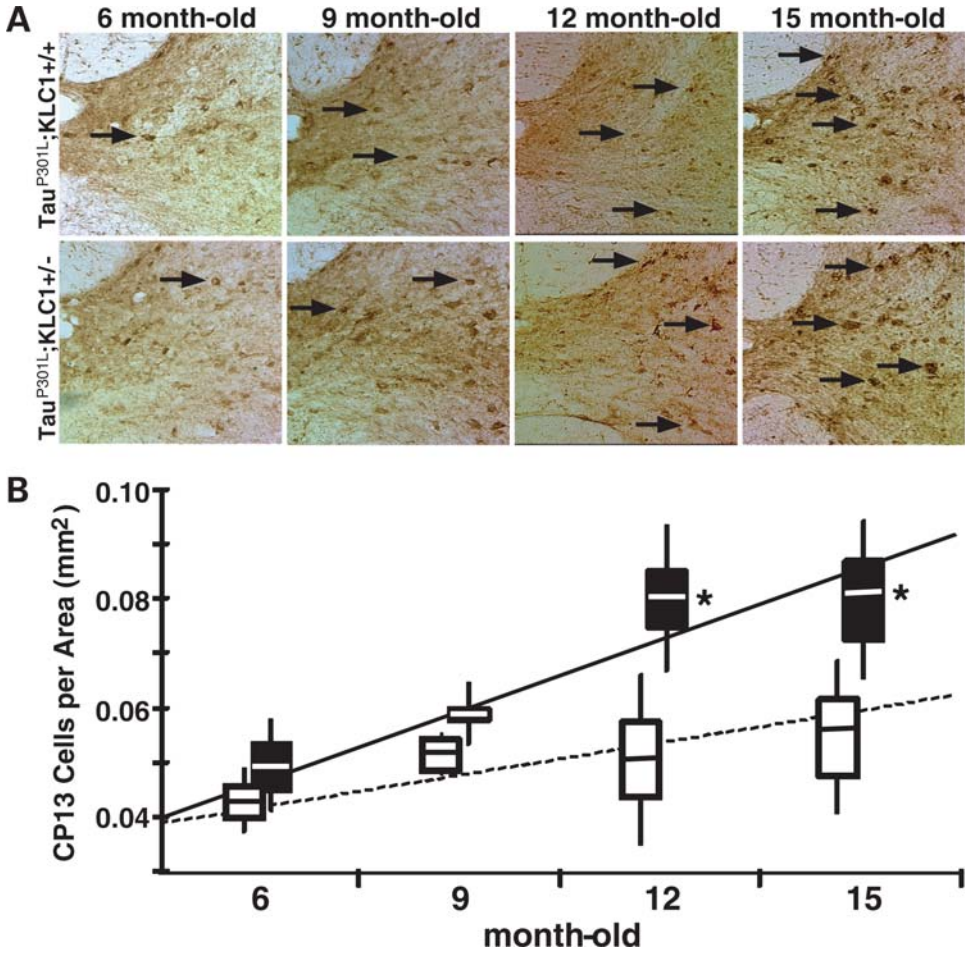

Figure 3. Increased cell body pathology in spinal cords of KLC1 reduction combined with tau P301L. (**A**) Staining of cervical spinal cord for phosphorylated tau at Ser-202 using CP13 antibody. p-tau accumulation in cell bodies of neurons from ventral regions of the spinal cord (arrows) at 6-, 9-, 12- and 15-month-old tau^{P301L};KLC1+/+ and tau^{P301L};KLC1+/− mice. (**B**) Stereological quantification of neuron number showing phosphorylated tau cell body accumulation in the gray matter areas for tau^{P301L};KLC1+/+ (27) and tau^{P301L};KLC1+/− (black). Regression line was plotted using average number. Boxes and bars correspond to SEM and STDEV, respectively. Mann–Whitney, non-parametric test; $n = 4$, $^{*}P < 0.05$).

Spinal cord analysis of the tau^{P301L} mouse revealed primarily insoluble filamentous accumulations with significant spinal neuronal loss and progressive motor disturbance (22). Similar to what we observed in the brain, KLC1 reduction in the spinal cord exacerbated the accumulation of insoluble tau in sarkosyl extractions performed at 12 months of age (Fig. 5A). Comparable to the brain, age-dependent increases in 64 kDa insoluble hyperphosphorylated tau were observed and quantified in sarkosyl extractions from 12-month-old tau^{P301L};KLC1+/− compared with tau^{P301L};KLC1+/− spinal cords (Fig. 5B). Taken together, these results suggest that with age, transport reduction can increase the pathological accumulation of insoluble hyperphosphorylated tau. Thus, transport defects can exacerbate tau-mediated neurodegeneration, a key process in the progression of many neurodegenerative tauopathies.

DISCUSSION

Abnormal tau hyperphosphorylation is an early and critical event in the pathogenesis of AD and other tauopathies as it may converge on impaired microtubule stability and/or aggregated filamentous species. Both phenomena may impair axonal transport (36). In AD, APP mutations and overexpression can cause transport defects that are independent of amyloid toxicity (37,38). Moreover, impairing the transport machinery can exacerbate AD-related pathologies, such as early axonopathies and amyloid deposition (39). The recent suggestion that transport defects can initiate biochemical events leading to abnormal tau behavior via JNK pathway activation (26) is also supported by the current study. A reduction in kinesin-1 anterograde motor function can exacerbate abnormal behavior of human tau in animal models of tauopathies. These results suggest that pathological cellular mechanisms that may initiate sporadic neurodegenerative tauopathies might also be enhanced by reduced rates of axonal transport. Moreover, transport reduction may also exacerbate the pathological accumulation, insoluble aggregation and neurodegeneration observed during the progression of tauopathies.

Different animal models of tauopathies have been instrumental in understanding the biochemical changes that occur in disease (23,40). Our and others experiments in *Drosophila*

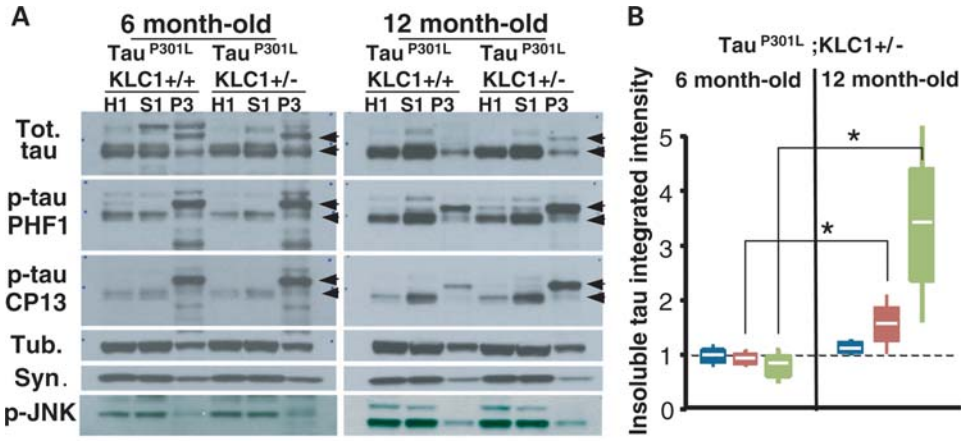

Figure 4. Transport reduction exacerbates insoluble tau accumulation in the brain stem. (**A**) Western blots showing total (Tot.) and phosphorylated forms of tau (PHF1, CP13) in homogenate (H1), soluble (S1) and insoluble (P3) fractions after sarkosyl extraction from brain stem of tau^{P301L};KLC1+/+ and tau^{P301L};KLC1+/− at 6- and 12-month-old mice. Tubulin (Tub.) and synuclein (Syn.) were used as loading controls. Arrows indicate tau shifts from 51 to 64 kDa. (**B**) Quantification of three different sarkosyl extractions each corresponding to two pooled mouse brain stems showing tau^{P301L};KLC1+/− normalized ratios of insoluble to homogenate (P3/H1) for total tau (blue), PHF1 (red) and CP13 (green) at 6- and 12-month-old mice. tau^{P301L};KLC1+/+ levels were considered as 1. White line, boxes and bars correspond to average, SEM and STDEV, respectively. Mann–Whitney, non-parametric test; $n = 6$, $^*P < 0.05$).

overexpressing wild-type and mutant tau suggest that tau alone can be detrimental to neuronal cells in the absence of any apparent toxic filament formation (20). Our finding that KLC reduction enhances neuronal tau accumulation and hyperphosphorylation in tau^{wt} or tau^{R406W} transgenic animals suggest that transport impairments can exacerbate tau-dependent loss of function phenotypes. One interesting possibility is that elevated neuronal microtubule destabilization may underlie the enhanced mortality observed in our *Drosophila* survival analyses. In addition, tau^{P301L} overexpression in mouse neurons recapitulates the generation of human neurofibrillary pathology such as insoluble tau deposits (22,32,41). Our sarkosyl extractions from tau^{P301L} tissue with KLC1 reductions revealed increased age-dependent deposition of pathological tau enriched in 64 kDa insoluble forms associated with abnormal filaments (33). Taken together, these data suggest that kinesin-1 axonal transport defects enhance tau pathological gain and loss of function leading to increased neurodegeneration.

Strong immunoreactivity for p-JNK has been observed in neurons containing hyperphosphorylated tau, as well as in dystrophic neurites of senile plaques in AD (26,42,43). Local JNK activation can influence tubulin assembly by modifying the affinity between tau and microtubules (44,45). This deregulation in the stress kinase pathway observed as p-JNK deposits precedes the formation of tau inclusions (46,47). Axonal injury or damage also induces the rapid phosphorylation of JNK and this process might be related to the initiation of retrograde damage signals traveling back to the cell body (48,49). In addition, activated JNK may stimulate retrograde transport-dependent signaling by direct phosphorylation of motor proteins (50,51). However, the molecular mechanisms that induce the initial stress kinase response in AD remain elusive. We recently suggested that early kinesin-1 transport defects can initiate the activation of different JNK isoforms (26). We now show that kinesin-1 transport impairments by KLC1 reduction can activate kinase pathways and enhance the hyperphosphorylation and insoluble aggregation of human wild-type and mutated tau. In the adult *Drosophila* brain, reducing KLC led to increased JNK activity together with tau stabilization and hyperphosphorylation. KLC1 reduction in tau^{P301L} mice enhances both p46 and p54 JNK phosphorylation suggesting that kinase pathways leading to elevated neurodegeneration can be exacerbated through impaired transport mechanisms.

In AD, axonal transport impairments have been implicated in the accumulation of synaptic defects and tangle pathology, which appears to commence distally and then spread retrogradely to the perikaryon (6,52). Tau overexpression may contribute to these defects by inhibiting anterograde transport along microtubules and impairing the synaptic delivery of vesicles and organelles (17,53). Mechanistically, changes in the amount of tau associated with microtubules might regulate the axonal transport machinery by exerting differential modulation of kinesin and dynein motility (18,54). However, it has been suggested recently that tau filaments rather than monomers may impair kinesin-dependent fast axonal transport by stimulating signaling pathways in disease (15). Alternatively, tau transport may also depend on molecular motors and tau phosphorylation states might regulate tau transport by differential interaction with the KLC1 subunit (19). Our finding of increased axonal aggregation and cell body accumulation of tau in *Drosophila* and mice suggest that tau transport might also be impaired after reducing the KLC1 motor subunit. By inducing kinesin-1 transport defects in tau models, we have enhanced a degeneration loop by selective stress kinase activation inducing higher tau phosphorylation but also by impairing kinesin-1-dependent tau movement.

Based on our results, it seems likely that cellular pathways that impair transport may increase the development of hyperphosphorylation and neurofibrillary pathology, inevitably leading to exacerbation of neurodegeneration. Based on the lack of neurodegeneration in APP and PSAPP mouse models (55–57), it seems likely that amyloid deposition does not lead to neuronal cell death in AD, and neurodegeneration requires a secondary or alternative process. This observation

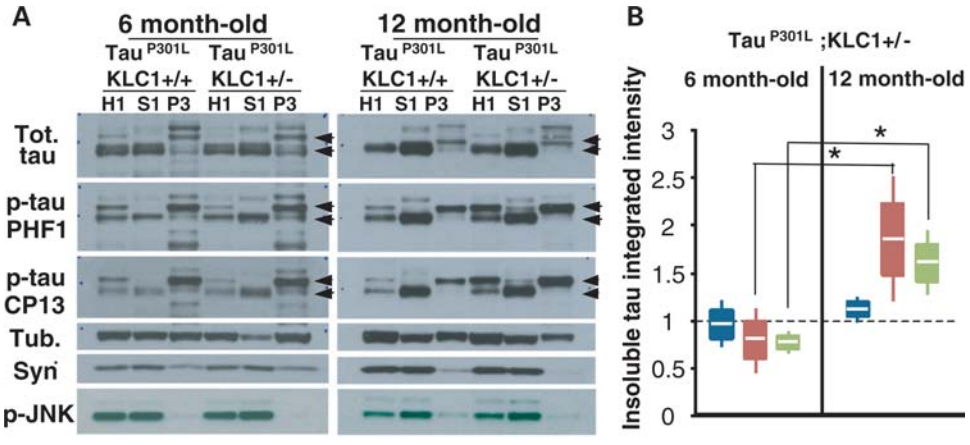

Figure 5. Transport reduction exacerbates insoluble tau accumulation in the spinal cord. (**A**) Westerns blots showing total (Tot.) and phosphorylated forms of tau (PHF1, CP13) in homogenate (H1), soluble (S1) and insoluble (P3) fractions after sarkosyl extraction from cervical spinal cord of tau^{P301L};KLC1+/+ and tau^{P301L};KLC1+/− at 6- and 12-month-old mice. Tubulin (Tub.) and synuclein (Syn.) were used as loading controls. Arrows indicate tau shifts from 51 to 64 kDa. (**B**) Quantification of three different sarkosyl extractions each corresponding to two pooled mouse cervical spinal cords showing tau^{P301L};KLC1+/− normalized ratios of insoluble to homogenate (P3/H1) for total tau (blue), PHF1 (red) and CP13 (green) at 6- and 12-month-old mice. tau^{P301L};KLC1+/+ levels were normalized to 1. White line, boxes and bars correspond to average, SEM and STDEV, respectively. Mann–Whitney, non-parametric test; $n = 6$, $^*P < 0.05$).

is consistent with studies describing no correlation between amyloid deposition and neuronal loss in AD (52). However, it has been suggested that APP overexpression alone can impair kinesin-1-dependent transport (37,39), which could initiate kinase activation and lead to abnormal tau hyperphosphorylation and NFT development (26). These two tau pathological characteristics have been closely correlated with neurodegeneration in AD (52). Therefore, we suggest that axonal transport defects can initiate neurodegeneration and/or exacerbate human tau-dependent disease pathways in AD and other neurodegenerative tauopathies.

MATERIALS AND METHODS

Drosophila

Human tau transgenic lines (20) carrying UAS driving tau^{wt} or tau^{R406W} were maintained as stocks at 25°C. For IF experiments, the panneuronal driver ApplGal4 (27) was used to induce expression of transgenes UAS-tau^{wt} or UAS-tau^{R406W} by crossing males transgenic animals to ApplGal4 females at 29°C. Females bearing the genotype ApplGal4/+;UAS-tau^{wt} or ApplGal4/+;UAS-tau^{R406W} were used. Survival and adult tau expression analyses in a KLC reduction background were done by crossing virgin UAS-tau^{wt} or UAS-tau^{R406W} females to ApplGal4;klc^{8ex94}/T(2:3)B3 CyO TM6B, Tb males at 25°C. The klc^{8ex94} allele bears a deletion in the third chromosome spanning the *KLC* gene (58). Female survival ratio was calculated by taking the number of progeny obtained with the genotype ApplGal4;klc^{8ex94}/UAS-$tau^{wt\ or\ R406W}$ and dividing it by the number of progeny obtained with the genotype ApplGal4;B3/UAS-$tau^{wt\ or\ R406W}$. The ratio from males without the ApplGal4 driver was obtained by dividing the number of +/Y; klc^{8ex94}/UAS-$tau^{wt\ or\ R406W}$ by +/Y;T(2,3)B3/UAS-$tau^{wt\ or\ R406W}$. Data were normalized to the female and male ratios obtained from ApplGal4; klc^{8ex94}/T(2:3)B3 crossed to wild-type flies. F1 males were used as negative controls in these experiments since they do not express tau.

Mice

JNPL3 males bearing two copies of the human tau P301L mutation driven by the prion promoter in a C57BL/6, DBA/2 strain were obtained from Taconic. Homozygous males were crossed to KLC1+/− females in a pure C57BL/6J background to obtain the experimental cohort of tau^{P301L};KLC1+/+ and tau^{P301L};KLC1+/− in a DBA/C57BL mixed background. Genotyping was performed by two PCR amplification reactions, one for human tau gene using specific primers and the other for KLC1 wild-type and recombinant alleles (26).

Antibodies

The following monoclonal antibodies were used: tubulin (Sigma); *Drosophila* syntaxin (Hybridoma bank), α-synuclein and JNK1/2 (BD biosciences). Polyclonal antibodies included: p-JNK (Cell Signaling). We also used the following anti-tau antibodies: TAU-5 (Biosource); tot-tau (Sigma); anti-p-tau: PHF1 and CP13 from P. Davies (Albert Einstein College of Medicine, NY, USA).

Drosophila experiments

Females bearing the genotype ApplGal4/+;UAS-tau^{wt} or tau^{R406W} were used for IF experiments. Briefly, larvae were dissected and probed with synaptotagmin (a kind gift from Hugo Bellen) and tau (a kind gift from Peter Davies) antibodies before images were taken on a BioRad confocal as described previously (37). For westerns, each lane was loaded using 10 μg of protein obtained from 12 adults heads homogenized in the lysis buffer (10 mM Tris–HCl, pH 7.4, 0.8 M NaCl, 1 mM EGTA, 0.1% Triton X-100, protease and

phosphatase inhibitors) at 4°C. Homogenates were centrifuged for 10 min at 10 000*g* at 4°C and supernatants from this spin were quantified for protein concentration. Protein quantification in westerns was performed using fluorescent-labeled secondary antibodies as previously described (26).

Brain and spinal cord dissection

At different ages, mice were transcardially perfused with 0.1 M Sorensen's phosphate buffer pH 7.2, dissected and flash frozen in dry ice for biochemistry. Tissues for immunohistochemistry were later fixed by immersion in 4% paraformaldehyde in Sorensen's buffer (4% PFA) (26) overnight at 4°C, and cryopreserved in 20% sucrose/dH_2O. Fifty micrometer sections from brain or spine were obtained using a Cryocut 1800 (Leica) at −19°C (59).

Histology and immunohistochemistry

Prior to immunohistochemistry stainings (59), tissue was quenched with 0.6% hydrogen peroxide followed by blocking. Signal was enhanced using a biotinylated secondary antibody and streptavidin using ABC vectastain kit, followed by Novared or DAB developing kits (Vector Labotratories).

Stereology

Stereology measurements were obtained with a Zeiss Axioplan light microscope equipped with a Bioquant Nova image analysis system (Bioquant R&M Biometrics, Inc.). In brief, the number of cell bodies with obvious pathology was estimated using the optical dissector method, $N=\Sigma Q^{-}$ (1/ssf)(1/asf)(1/tsf) (60). Random serial sections were analyzed using Bioquant. Criteria for profile counting required that staining exhibited positive CP13 cell body morphological features consistent with neurons. For spinal cord, all CP13 positive abnormal cell bodies in gray matter were counted.

Statistical analysis

Average, standard error of the mean (SEM) and standard deviation (STDEV) are plotted in the graphs. Asterisks indicate significance. For brain and spinal cord stereology, non-parametric statistical tests were used. As indicated, Student's *t*-test, one-way Kruskal–Wallis test or Mann–Whitney (two sample rank sum) test was used to analyze fluorescence intensity of secondary antibodies, CP13 cell bodies in the brain and spinal cord, and the integrated intensity of westerns. A population percentage distribution chi-square test was used to analyze progeny obtained from *Drosophila* crosses.

Protein quantification

Secondary fluorescent-labeled antibodies were used in westerns for quantification. SDS–PAGE protein gels were transferred to nitrocellulose, blocked and washes were performed in the absence of Tween detergent to decrease background. Secondary antibodies coupled to 800 and 700 nm infrared fluorophores were used in combination to detect levels of p-JNK and total JNK on the same membrane. Protein concentration curves were loaded and secondary antibodies used to define respective antibody affinities and the range of linear detection. An Odyssey imaging system (Li-Cor) was used to measure fluorescence intensity.

Sarkosyl soluble and insoluble extractions

Briefly, brain cortex, stem and spinal cord were harvested, weighted and homogenized using a teflon-glass homogenizer attached to a labo-stirrer (Yamato) in three volumes of the TBS buffer consisting of 25 mM Tris–HCl (pH 7.4), 150 mM NaCl, 1 mM EGTA, 1 mM EDTA, protease inhibitor cocktail (61) and phosphatase inhibitors (10 μM sodium fluoride, 1 mM sodium orthovanadate) (62,63). Homogenates were centrifuged for 15 min at 150 000*g* at 4°C. Supernatants were collected as the soluble fraction and pellets were re-homogenized in three volumes of the Salt/Sucrose buffer consisting of 0.8 M NaCl, 10% sucrose, 10 mM Tris–HCl (pH 7.4), 1 mM EGTA, protease inhibitor cocktail, and phosphatase inhibitors and later centrifuged for 15 min at 150 000*g* at 4°C. Supernatants from this spin were incubated with 1% N-laurylsarcosinate (sarkosyl) at 37°C for 1 h with moderate shaking. Sarkosyl solution was centrifuged at 150 000*g* for 30 min at 4°C, and sarkosyl-insoluble pellets resuspended in protein loading buffer by similar weight/volume ratio. Protein concentrations were determined and SDS–PAGE protein gels ran for western blot analysis. The same amount of protein was loaded in homogenates and soluble supernatant immunoblots, and sarkosyl-insoluble pellets were loaded using similar weight/volume ratio.

SUPPLEMENTARY MATERIAL

Supplementary Material is available at *HMG* online.

ACKNOWLEDGEMENTS

We thank Dr Peter Davies for providing tau antibodies; Ximena Pastorino for constant support; Drs Almenar-Queralt, Encalada, Schimmelpfeng, Weaver, Duncan, Bache, Shah and all members of the Goldstein laboratory.

Conflict of Interest statement. None declared.

FUNDING

This work was supported by the National Institute of Health (Grants numbers GM35252 and AG032180 to L.S.B.G.); the Pew Latin American Program and the American Parkinson Disease Association (T.L.F.); the Ellison Medical Foundation senior postdoctoral fellowship and new investigator grant from the Alzheimer Association (S.G.). L.S.B.G. is an investigator of the Howard Hughes Medical Institute.

REFERENCES

1. Ballatore, C., Lee, V.M. and Trojanowski, J.Q. (2007) Tau-mediated neurodegeneration in Alzheimer's disease and related disorders. *Nat. Rev. Neurosci.*, **8**, 663–672.

2. Lee, V.M., Goedert, M. and Trojanowski, J.Q. (2001) Neurodegenerative tauopathies. *Annu. Rev. Neurosci.*, **24**, 1121–1159.
3. Alonso, A.C., Li, B., Grundke-Iqbal, I. and Iqbal, K. (2008) Mechanism of tau-induced neurodegeneration in Alzheimer disease and related tauopathies. *Curr. Alzheimer Res.*, **5**, 375–384.
4. De Vos, K.J., Grierson, A.J., Ackerley, S. and Miller, C.C. (2008) Role of axonal transport in neurodegenerative diseases. *Annu. Rev. Neurosci.*, **31**, 151–173.
5. Higuchi, M., Lee, V.M. and Trojanowski, J.Q. (2002) Tau and axonopathy in neurodegenerative disorders. *Neuromolecular Med.*, **2**, 131–150.
6. Su, J.H., Deng, G. and Cotman, C.W. (1997) Transneuronal degeneration in the spread of Alzheimer's disease pathology: immunohistochemical evidence for the transmission of tau hyperphosphorylation. *Neurobiol. Dis.*, **4**, 365–375.
7. Xie, S., Xiao, J.X., Gong, G.L., Zang, Y.F., Wang, Y.H., Wu, H.K. and Jiang, X.X. (2006) Voxel-based detection of white matter abnormalities in mild Alzheimer disease. *Neurology*, **66**, 1845–1849.
8. Hutton, M., Lendon, C.L., Rizzu, P., Baker, M., Froelich, S., Houlden, H., Pickering-Brown, S., Chakraverty, S., Isaacs, A., Grover, A. *et al.* (1998) Association of missense and 5′-splice-site mutations in tau with the inherited dementia FTDP-17. *Nature*, **393**, 702–705.
9. Poorkaj, P., Bird, T.D., Wijsman, E., Nemens, E., Garruto, R.M., Anderson, L., Andreadis, A., Wiederholt, W.C., Raskind, M. and Schellenberg, G.D. (1998) Tau is a candidate gene for chromosome 17 frontotemporal dementia. *Ann. Neurol.*, **43**, 815–825.
10. Spillantini, M.G., Murrell, J.R., Goedert, M., Farlow, M.R., Klug, A. and Ghetti, B. (1998) Mutation in the tau gene in familial multiple system tauopathy with presenile dementia. *Proc. Natl Acad. Sci. USA*, **95**, 7737–7741.
11. Buee, L., Bussiere, T., Buee-Scherrer, V., Delacourte, A. and Hof, P.R. (2000) Tau protein isoforms, phosphorylation and role in neurodegenerative disorders. *Brain Res. Brain Res. Rev.*, **33**, 95–130.
12. Gasparini, L., Terni, B. and Spillantini, M.G. (2007) Frontotemporal dementia with tau pathology. *Neurodegener. Dis.*, **4**, 236–253.
13. Bramblett, G.T., Goedert, M., Jakes, R., Merrick, S.E., Trojanowski, J.Q. and Lee, V.M. (1993) Abnormal tau phosphorylation at Ser396 in Alzheimer's disease recapitulates development and contributes to reduced microtubule binding. *Neuron*, **10**, 1089–1099.
14. Lindwall, G. and Cole, R.D. (1984) Phosphorylation affects the ability of tau protein to promote microtubule assembly. *J. Biol. Chem.*, **259**, 5301–5305.
15. LaPointe, N.E., Morfini, G., Pigino, G., Gaisina, I.N., Kozikowski, A.P., Binder, L.I. and Brady, S.T. (2009) The amino terminus of tau inhibits kinesin-dependent axonal transport: implications for filament toxicity. *J. Neurosci. Res.*, **87**, 440–451.
16. Goldstein, L.S. (2003) Do disorders of movement cause movement disorders and dementia? *Neuron*, **40**, 415–425.
17. Stamer, K., Vogel, R., Thies, E., Mandelkow, E. and Mandelkow, E.M. (2002) Tau blocks traffic of organelles, neurofilaments, and APP vesicles in neurons and enhances oxidative stress. *J. Cell Biol.*, **156**, 1051–1063.
18. Dixit, R.R.J., Goldman, Y.E. and Holzbaur, E.L. (2008) Differential regulation of dynein and kinesin motor proteins by tau. *Science*, **319**, 1086–1089.
19. Cuchillo-Ibanez, I., Seereeram, A., Byers, H.L., Leung, K.Y., Ward, M.A., Anderton, B.H. and Hanger, D.P. (2008) Phosphorylation of tau regulates its axonal transport by controlling its binding to kinesin. *FASEB J.*, **22**, 3186–3195.
20. Wittmann, C.W., Wszolek, M.F., Shulman, J.M., Salvaterra, P.M., Lewis, J., Hutton, M. and Feany, M.B. (2001) Tauopathy in *Drosophila*: neurodegeneration without neurofibrillary tangles. *Science*, **293**, 711–714.
21. Khurana, V. (2008) Modeling Tauopathy in the fruit fly *Drosophila* melanogaster. *J. Alzheimers Dis.*, **15**, 541–553.
22. Lewis, J., McGowan, E., Rockwood, J., Melrose, H., Nacharaju, P., Van Slegtenhorst, M., Gwinn-Hardy, K., Paul Murphy, M., Baker, M., Yu, X. *et al.* (2000) Neurofibrillary tangles, amyotrophy and progressive motor disturbance in mice expressing mutant (P301L) tau protein. *Nat. Genet.*, **25**, 402–405.
23. McGowan, E., Eriksen, J. and Hutton, M. (2006) A decade of modeling Alzheimer's disease in transgenic mice. *Trends Genet.*, **22**, 281–289.
24. Higuchi, M., Zhang, B., Forman, M.S., Yoshiyama, Y., Trojanowski, J.Q. and Lee, V.M. (2005) Axonal degeneration induced by targeted expression of mutant human tau in oligodendrocytes of transgenic mice that model glial tauopathies. *J. Neurosci.*, **25**, 9434–9443.
25. Bearer, E.L., Falzone, T.L., Zhang, X., Biris, O., Rasin, A. and Jacobs, R.E. (2007) Role of neuronal activity and kinesin on tract tracing by manganese-enhanced MRI (MEMRI). *Neuroimage*, **37**, S37–S46.
26. Falzone, T.L., Stokin, G.B., Lillo, C., Rodrigues, E.M., Westerman, E.L., Williams, D.S. and Goldstein, L.S. (2009) Axonal stress kinase activation and tau misbehavior induced by kinesin-1 transport defects. *J. Neurosci.*, **29**, 5758–5767.
27. Torroja, L., Chu, H., Kotovsky, I. and White, K. (1999) Neuronal overexpression of APPL, the *Drosophila* homologue of the amyloid precursor protein (APP), disrupts axonal transport. *Curr. Biol.*, **9**, 489–492.
28. Su, J.H., Cummings, B.J. and Cotman, C.W. (1994) Early phosphorylation of tau in Alzheimer's disease occurs at Ser-202 and is preferentially located within neurites. *Neuroreport*, **5**, 2358–2362.
29. Goedert, M., Jakes, R., Crowther, R.A., Six, J., Lubke, U., Vandermeeren, M., Cras, P., Trojanowski, J.Q. and Lee, V.M. (1993) The abnormal phosphorylation of tau protein at Ser-202 in Alzheimer disease recapitulates phosphorylation during development. *Proc. Natl Acad. Sci. USA*, **90**, 5066–5070.
30. Lin, W.L., Zehr, C., Lewis, J., Hutton, M., Yen, S.H. and Dickson, D.W. (2005) Progressive white matter pathology in the spinal cord of transgenic mice expressing mutant (P301L) human tau. *J. Neurocytol.*, **34**, 397–410.
31. Ramsden, M., Kotilinek, L., Forster, C., Paulson, J., McGowan, E., SantaCruz, K., Guimaraes, A., Yue, M., Lewis, J., Carlson, G. *et al.* (2005) Age-dependent neurofibrillary tangle formation, neuron loss, and memory impairment in a mouse model of human tauopathy (P301L). *J. Neurosci.*, **25**, 10637–10647.
32. Deters, N., Ittner, L.M. and Gotz, J. (2008) Divergent phosphorylation pattern of tau in P301L tau transgenic mice. *Eur. J. Neurosci.*, **28**, 137–147.
33. Sahara, N., Lewis, J., DeTure, M., McGowan, E., Dickson, D.W., Hutton, M. and Yen, S.H. (2002) Assembly of tau in transgenic animals expressing P301L tau: alteration of phosphorylation and solubility. *J. Neurochem.*, **83**, 1498–1508.
34. Kampers, T., Pangalos, M., Geerts, H., Wiech, H. and Mandelkow, E. (1999) Assembly of paired helical filaments from mouse tau: implications for the neurofibrillary pathology in transgenic mouse models for Alzheimer's disease. *FEBS Lett.*, **451**, 39–44.
35. Lewis, J., Dickson, D.W., Lin, W.L., Chisholm, L., Corral, A., Jones, G., Yen, S.H., Sahara, N., Skipper, L., Yager, D. *et al.* (2001) Enhanced neurofibrillary degeneration in transgenic mice expressing mutant tau and APP. *Science*, **293**, 1487–1491.
36. Stokin, G.B. and Goldstein, L.S. (2006) Axonal transport and Alzheimer's disease. *Annu. Rev. Biochem.*, **75**, 607–627.
37. Gunawardena, S. and Goldstein, L.S. (2001) Disruption of axonal transport and neuronal viability by amyloid precursor protein mutations in *Drosophila*. *Neuron*, **32**, 389–401.
38. Stokin, G.B., Almenar-Queralt, A., Gunawardena, S., Rodrigues, E.M., Falzone, T., Kim, J., Lillo, C., Mount, S.L., Roberts, E.A., McGowan, E. *et al.* (2008) Amyloid precursor protein-induced axonopathies are independent of amyloid-beta peptides. *Hum. Mol. Genet.*, **17**, 3474–3486.
39. Stokin, G.B., Lillo, C., Falzone, T.L., Brusch, R.G., Rockenstein, E., Mount, S.L., Raman, R., Davies, P., Masliah, E., Williams, D.S. *et al.* (2005) Axonopathy and transport deficits early in the pathogenesis of Alzheimer's disease. *Science*, **307**, 1282–1288.
40. Gotz, J. and Ittner, L.M. (2008) Animal models of Alzheimer's disease and frontotemporal dementia. *Nat. Rev. Neurosci.*, **9**, 532–544.
41. Probst, A., Gotz, J., Wiederhold, K.H., Tolnay, M., Mistl, C., Jaton, A.L., Hong, M., Ishihara, T., Lee, V.M., Trojanowski, J.Q. *et al.* (2000) Axonopathy and amyotrophy in mice transgenic for human four-repeat tau protein. *Acta Neuropathol. (Berl.)*, **99**, 469–481.
42. Ferrer, I., Blanco, R., Carmona, M. and Puig, B. (2001) Phosphorylated mitogen-activated protein kinase (MAPK/ERK-P), protein kinase of 38 kDa (p38-P), stress-activated protein kinase (SAPK/JNK-P), and calcium/calmodulin-dependent kinase II (CaM kinase II) are differentially expressed in tau deposits in neurons and glial cells in tauopathies. *J. Neural. Transm.*, **108**, 1397–1415.
43. Pei, J.J., Braak, E., Braak, H., Grundke-Iqbal, I., Iqbal, K., Winblad, B. and Cowburn, R.F. (2001) Localization of active forms of C-jun kinase (JNK) and p38 kinase in Alzheimer's disease brains at different stages of neurofibrillary degeneration. *J. Alzheimers Dis.*, **3**, 41–48.

44. Goedert, M., Hasegawa, M., Jakes, R., Lawler, S., Cuenda, A. and Cohen, P. (1997) Phosphorylation of microtubule-associated protein tau by stress-activated protein kinases. *FEBS Lett.*, **409**, 57–62.
45. Yoshida, H., Hastie, C.J., McLauchlan, H., Cohen, P. and Goedert, M. (2004) Phosphorylation of microtubule-associated protein tau by isoforms of c-Jun N-terminal kinase (JNK). *J. Neurochem.*, **90**, 352–358.
46. Atzori, C., Ghetti, B., Piva, R., Srinivasan, A.N., Zolo, P., Delisle, M.B., Mirra, S.S. and Migheli, A. (2001) Activation of the JNK/p38 pathway occurs in diseases characterized by tau protein pathology and is related to tau phosphorylation but not to apoptosis. *J. Neuropathol. Exp. Neurol.*, **60**, 1190–1197.
47. Lagalwar, S., Guillozet-Bongaarts, A.L., Berry, R.W. and Binder, L.I. (2006) Formation of phospho-SAPK/JNK granules in the hippocampus is an early event in Alzheimer disease. *J. Neuropathol. Exp. Neurol.*, **65**, 455–464.
48. Cavalli, V., Kujala, P., Klumperman, J. and Goldstein, L.S. (2005) Sunday Driver links axonal transport to damage signaling. *J. Cell Biol.*, **168**, 775–787.
49. Neumann, H. (2003) Molecular mechanisms of axonal damage in inflammatory central nervous system diseases. *Curr. Opin. Neurol.*, **16**, 267–273.
50. Morfini, G., Pigino, G., Szebenyi, G., You, Y., Pollema, S. and Brady, S.T. (2006) JNK mediates pathogenic effects of polyglutamine-expanded androgen receptor on fast axonal transport. *Nat. Neurosci.*, **9**, 907–916.
51. Morfini, G.A., You, Y.M., Pollema, S.L., Kaminska, A., Liu, K., Yoshioka, K., Bjorkblom, B., Coffey, E.T., Bagnato, C., Han, D. *et al.* (2009) Pathogenic huntingtin inhibits fast axonal transport by activating JNK3 and phosphorylating kinesin. *Nat. Neurosci.*, **12**, 864–871.
52. Braak, H. and Braak, E. (1991) Neuropathological staging of Alzheimer-related changes. *Acta Neuropathol. (Berl.)*, **82**, 239–259.
53. Ebneth, A., Godemann, R., Stamer, K., Illenberger, S., Trinczek, B. and Mandelkow, E. (1998) Overexpression of tau protein inhibits kinesin-dependent trafficking of vesicles, mitochondria, and endoplasmic reticulum: implications for Alzheimer's disease. *J. Cell Biol.*, **143**, 777–794.
54. Trinczek, B., Ebneth, A., Mandelkow, E.M. and Mandelkow, E. (1999) Tau regulates the attachment/detachment but not the speed of motors in microtubule-dependent transport of single vesicles and organelles. *J. Cell Sci.*, **112**, 2355–2367.
55. Irizarry, M.C., McNamara, M., Fedorchak, K., Hsiao, K. and Hyman, B.T. (1997) APPSw transgenic mice develop age-related A beta deposits and neuropil abnormalities, but no neuronal loss in CA1. *J. Neuropathol. Exp. Neurol.*, **56**, 965–973.
56. Irizarry, M.C., Soriano, F., McNamara, M., Page, K.J., Schenk, D., Games, D. and Hyman, B.T. (1997) Abeta deposition is associated with neuropil changes, but not with overt neuronal loss in the human amyloid precursor protein V717F (PDAPP) transgenic mouse. *J. Neurosci.*, **17**, 7053–7059.
57. Takeuchi, A., Irizarry, M.C., Duff, K., Saido, T.C., Hsiao Ashe, K., Hasegawa, M., Mann, D.M., Hyman, B.T. and Iwatsubo, T. (2000) Age-related amyloid beta deposition in transgenic mice overexpressing both Alzheimer mutant presenilin 1 and amyloid beta precursor protein Swedish mutant is not associated with global neuronal loss. *Am. J. Pathol.*, **157**, 331–339.
58. Gindhart, J.G. Jr, Desai, C.J., Beushausen, S., Zinn, K. and Goldstein, L.S. (1998) Kinesin light chains are essential for axonal transport in *Drosophila*. *J. Cell Biol.*, **141**, 443–454.
59. Celis, J.E. (1994) *Cell Biology—A Laboratory Handbook.* Academic Press Ltd, San Diego, CA.
60. Long, J.M., Mouton, P.R., Jucker, M. and Ingram, D.K. (1999) What counts in brain aging? Design-based stereological analysis of cell number. *J. Gerontol. A Biol. Sci. Med. Sci.*, **54**, B407–B417.
61. Vermersch, P., Roche, J., Hamon, M., Daems-Monpeurt, C., Pruvo, J.P., Dewailly, P. and Petit, H. (1996) White matter magnetic resonance imaging hyperintensity in Alzheimer's disease: correlations with corpus callosum atrophy. *J. Neurol.*, **243**, 231–234.
62. Dickey, C.A., Yue, M., Lin, W.L., Dickson, D.W., Dunmore, J.H., Lee, W.C., Zehr, C., West, G., Cao, S., Clark, A.M. *et al.* (2006) Deletion of the ubiquitin ligase CHIP leads to the accumulation, but not the aggregation, of both endogenous phospho- and caspase-3-cleaved tau species. *J. Neurosci.*, **26**, 6985–6996.
63. Gotz, J., Chen, F., van Dorpe, J. and Nitsch, R.M. (2001) Formation of neurofibrillary tangles in P301l tau transgenic mice induced by Abeta 42 fibrils. *Science*, **293**, 1491–1495.